Entropy Generation on Thermal Transfer in MHD Natural Convection of Cu – H_2O Nanofluid in a Porous Medium with Heat Generation/Absorption

Achogo, Wisdom Hezekiah[1], Eleonu, Blessing Chikaodi[2], Nnoka, Love Cherukei[3]

[1]*Department of Mathematics/Statistics, Ignatius Ajuru University of Education, P.M.B 5047 Rumuolumeni, Nigeria*

[2,3]*Department of Mathematics/Statistics, Captain Elechi Amadi Polytechnic Rumuola, P.M.B 5936 Port Harcourt, Nigeria*

Abstract: **The study investigated entropy generation on thermal transfer in MHD natural convection of Cu-H_2O nanofluid in a porous medium with heat generation/absorption. A set of partial differential equations with copper nanoparticles were used. The partial differential equations were non-dimensioned with various dimensionless quantities in order to obtain forms whose solutions can be easily obtained. The partial differential equations were later transformed into ordination differential equations through a two term perturbation technique which were later solved using method of undetermined coefficient to obtain the exact solutions for the energy and momentum equations. The exact solutions for momentum and energy were later used to estimate the entropy generation. Using the exact solutions; plots were done with the aid of standard parameters to estimate the variational effects of parameters that entered the flow field and from the plots; it was observed that thermal radiation decreased the temperature of the fluid. Heat generation/absorption parameter increased the temperature of the fluid. The effective thermal conductivity increased the temperature of the fluid. Peclet number decreased the velocity of the fluid. Reynolds number decreased the fluid velocity. Peclet number, Reynolds number and heat generation rapidly increased and decreased the entropy generation at the lower and upper plates respectively.**

Keywords: **Entropy generation, Nanofluid, Magnetohydrodynamics (MHD)**

I. INTRODUCTION

Thermal conductivity plays a vital role in warmness transfer enhancement. Conventional heat switch fluids along with water, ethylene glycol (EG), kerosene oil and lubricant oils have negative thermal conductivities compared to solids. Solids debris however have better thermal conductivities in comparison to traditional warmth switch fluids. Choi (1995) in his pioneering paintings indicated that when a small quantity of nanoparticles .is added to not unusual base fluids, it will increase extensively the thermal conductivity of the base fluids in addition to their convective warmness transfer rate. This combination is known as nanofluids. More precisely, nanofluids are suspensions of nano-length debris in base fluids. Usually nanofluids include specific sorts of nanoparticles inclusive of oxides, metals and carbides in generally base fluids like water, EG, propylene glycol and kerosene oil. Some unique packages of nanofluids are located in various digital equipment, energy supply, energy generation, air con and manufacturing. Vajjha and Das (2009) for the first time used EG (60 %) and water (forty %) aggregate as base fluid for the preparation of alumina (Al_2O_3), copper oxide (CuO) and zinc oxide (ZnO) nanofluids. At the identical temperature and attention, they observed that CuO nanofluid possess excessive thermal conductivity evaluate to the ones of Al2O3 and ZnO nanofluids. Naik and Sundar (2011) took 70 % propylene glycol and 30 % water and prepared CuO nanofluid. As expected, they found that CuO nanofluid has better thermal conductivity and viscosity homes compare to base fluid. Malvandi et al.(2013) studied entropy generation of nanofluids over a plate analytically. The used the homotopy-pertubation method(HPM) and the variational iteration method(VIM) to solve the nonlinear ordinary differential equation. It was noted the high density of Cu adding this nanoparticles to water generates more entropy in contrast to other nanoparticles in a process. Thiagarajan et al.(2019) embarked on the study viscous dissipation and joule heating effects on thermo solutal stratified nanofluid over a stretching sheet. They remarked that Schmidt number decreases the temperature after obtaining a numerical solution of the nonlinear ordinary differential equations. Md et al.(2012) studied the unsteady mhd free convection of nanofluid along a stretching sheet with thermal radiation. They obtained different time steps and for the different values of the parameters of physical and engineering interest. Natural convection flow of fractional nanofluids over an isothermal vertical plate with thermal radiation was studied by Constantin et al.(2017). The fluid temperature increases for increasing values of the nanoparticle volume fraction was noted by them after obtaining the closed form solution and plotting the graph. Latiff et al.(2016) studied Stefan blowing effect of nanofluid over a solid rotating stretchable disk. The nonlinear ordinary differential equations were solved numerically using the Runge-Kutta-Fehlberg method. It was remarked that the Stefan blowing increases the local skin friction and reduces the heat transfer, mass transfer and microorganism transfer rates. Second order slip flow of Cu-Water nanofluid over a stretching sheet with heat transfer was undergone by Rajesh et al.(2014). They solved the differential equations using finite element method. They show the effects of parameters variation with the aid of graphs. Aaiza et al.(2015) studied energy transfer in nanofluid containing different shapes of nanoparticles. They found that viscosity

and thermal conductivity ate the most prominent parameters responsible for different results of velocity and temperature.

The foundation of the knowledge of entropy technology goes to Clausius and Kelvins research on the irreversibility elements of the second law of thermodynamics. However, the entropy technology on account of temperature differences has remained untreated via classical thermodynamics. The 2nd law evaluation is important due to the fact it's far one of the methods used for predicting the overall performance of engineering processes. Since entropy generation is the measure of the destruction of available work of the system, the dedication of the energetic factors motivating the entropy generation is critical in upgrading the machine performances. Rapid progress in technological know-how and technology has caused the development of increasingly drift devices that involve the manipulation of fluid flow in numerous geometries. The production of thermal and engineering gadgets is involved by way of irreversible losses that result in increase in entropy and reduce gadget performance. Thus it is crucial to locate the elements that decrease the entropy era and maximize the flow machine efficiency. To analyze the irreversibilities inside the form of entropy generation, the second regulation of thermodynamics is applied. Factors which are liable for the irreversibility are heat transfer throughout finite temperature gradients, traits of convective warmness transfer and viscous dissipation. Most of the electricity associated applications consisting of cooling of present day electronic structures, solar electricity creditors, and geothermal strength systems depend upon entropy production. The concept of entropy generation has earned so much attention from several authors in the persons of Baag et al.(2019) who studied entropy generation over a stretching sheet for viscoelastic MHD flow. They solved the model analytically by adopting the Kummer's function. The striking the result they obtained is that Darcy dissipation favours higher level entropy generation in all the cases except the flow of liquid with low thermal diffusivity assuming the process to be irreversible. Entropy generation in a couple stress fluid flow was investigated by Makinde et al.(2013). The nonlinear governing equations were solved numerically using shooting methods together with a Runge-Kutta Fehlberge integration scheme. They noted that increasing Grashof number increases the entropy generation. Ajibade et al.(2011) studied entropy generation under the effect of suction/injection. The dimensionless differential equations were solved through method of undetermined coefficient analytically to obtain a closed form for the velocity, temperature. Entropy generation and Bejan number are extensively discussed the help of graphs. It was remarked that entropy generation number increases with suction on one porous plate while it decreased on the other porous plate with injection. Shateyi et al.(2015) studied spectral relaxation method for entropy generation on a mhd flow and heat transfer of a Maxwell fluid. They used the bvp4c and spectral methods to solve the nonlinear equations. They found out that spectral relaxation method was found to be accurate and rapidly convergent to the numerical results. Entropy generation in a micropolar fluid flow through an inclined channel was studied by Srinivasacharya et al.(2015). Thy solved the governing equations using the spectral quasilinearization method. they observed that the increase in coupling number, Prandtl number and Reynolds number reduces the entropy generation number.

Magnetohydrodynamics (MHD) is the science which is associated with the motion of exceedingly conducting liquids in the presence of a magnetic field. The motion of the conducting liquid throughout the magnetic area generates electric currents which change the magnetic field, and the motion of the magnetic field on those currents offers upward thrust to mechanical forces which alter the drift of the liquid. MHD combines both standards of fluid dynamics and electromagnetism. MHD considers the magnetic properties of electrically conducting fluids. When an electrically conducting fluid moves through a magnetic field, an electric field may be brought on and will interact with the magnetic properties to supply a body pressure. The science which deals with this phenomenon is referred to as magnetohydrodynamics. Soret effect on MHD free convection through a porous inclined channel was embarked upon by Achogo et al.(2020). They noted that soret number increases both the concentration and velocity profiles after obtaining the closed form analytically through the method of undetermined coefficient. Reddy et al.(2011) examined mass transfer and heat generation effects on MHD free convection flow past an inclined vertical surface ina porous medium. They solved the nonlinear systems through a numerical approach by applying the Runge-Kutta method of fourth order with shooting technique. Buggaramulu et al.(2017) studied MHD convection flow of Kuvshinski fluid past an infinite vertical porus plate. The nonlinear equations were solved by adopting a two term perturbation technique and they solved analytically.

In this research we considered entropy generation on thermal transfer of entropy generation on thermal transfer in MHD natural convection of $Cu - H_2O$ nanofluid in a porous medium with heat generation/absorption.

II. FORMULATION OF THE PROBLEM

The following assumptions were made;

a) The flow is oscillatory of nanofluids
b) The fluid is electrically conducting in the presence of uniform magnetic field applied perpendicularly to the direction of flow.
c) The magnetic Reynolds number is very small such that the impact of induced magnetic field is forfeited.
d) The external electric field is considered zero and the electric field due to polarization is negligible.
e) The no-slip condition at the boundary walls is considered.
f) The x-axis is taken along the flow and y-axis is taken normal to the direction of flow.

g) The natural convection results from buoyancy force together with external pressure gradient applied along the x-direction.
h) T_0 and T_w are considered very high enough to induce the radiative heat transfer.

i) Going by the Boussinesq approximation, the governing equations of momentum and energy are as follows;

$$\rho_{nf}\left(\frac{\partial u'}{\partial t'}+v'\frac{\partial u'}{\partial y'}\right)=-\frac{\partial p'}{\partial x'}+\mu_{nf}\frac{\partial^2 u'}{\partial y'^2}-\frac{\mu_{nf}}{K}u'-\sigma\beta_0^2u'+g(\rho\beta)_{nf}(T'-T_0) \quad (1)$$

$$\left(\rho c_p\right)_{nf}\left(\frac{\partial T'}{\partial t'}+v'\frac{\partial T'}{\partial y'}\right)=k_{nf}\frac{\partial^2 T'}{\partial y'^2}-\frac{\partial q_r'}{\partial y'}-Q_0(T'-T_0) \quad (2)$$

Where u=u(y,t) represents the velocity in the direction of x, T=T(y,t) the temperature, ρ_{nf} the density, μ_{nf} the dynamic viscosity of the nanofluid, σ the electrical conductivity of the base fluid, K> 0 the permeability of the porous medium, $(\rho\beta)_{nf}$ thermal expansion coefficient of nanofluid, g the acceleration due to gravity, $\left(\rho c_p\right)_{nf}$ the heat capacitance of nanofluids, k_{nf} the thermal conductivity of nanofluid, q_r the radiative heat flux in x-direction, p the external pressure, Q_0 the heat generation/absorption

The boundary condition expedient are as follows;

y=0; u=0, $T=T_0$ (3a)

y=d; u=0, $T=T_w$ (3b)

Following the Hamilton and Crosser model(1962),the dynamic viscosity of the nanofluid(μ_{nf}), thermal expansion coefficient of nanofluid($(\rho\beta)_{nf}$), heat capacitance of nanofluids($\left(\rho c_p\right)_{nf}$), thermal conductivity of nanofluid(k_{nf}) are;

$$\mu_{nf}=\mu_f(1+a\emptyset+b\emptyset^2) \quad (4a)$$

$$\frac{k_{nf}}{k_f}=\frac{k_s+(n-1)k_f+(n-1)(k_s-k_f)\emptyset}{k_s+(n-1)k_f+(k_s-k_f)\emptyset} \quad (4b)$$

$$\rho_{nf}=(1-\emptyset)\rho_f+\emptyset\rho_s \quad (4c)$$

$$(\rho\beta)_{nf}=(1-\emptyset)(\rho\beta)_f+\emptyset(\rho\beta)_s \quad (4d)$$

$$\left(\rho c_p\right)_{nf}=(1-\emptyset)\left(\rho c_p\right)_f+\emptyset\left(\rho c_p\right)_s \quad (4e)$$

$\emptyset$ denotes the nanoparticles volume fraction, ρ_f and ρ_s are the densities of the base fluid and solid nanoparticles, β_s and β_f are the volumetric expansion coefficients of thermal expansions of solid nanopartiles and base fluids,$\left(c_p\right)_s$ and $\left(c_p\right)_f$ are the specific heat capacities of solid nanoparticles and base fluids at constant pressure, a and b represent constants and find their values on the particle shape as represented by Aaiza et al.(2015) in Table 1. The n in equation (4b) denotes the empirical shape factor and it is expressed as $n=\frac{3}{\Psi}$, where Ψ means the sphericity which denotes the ratio between the surface are of the sphere and the surface area of the real particle with equal volumes(Aiza et al.(2015)). The Ψ is clearly seen in Table 2.

Table1: Constants a and b empirical shape factors

Model	Platelet	Blade	Cylinder	Brick
A	37.1	14.6	13.5	1.9
B	612.6	123.3	904.4	471.4

Table 2: Sphericity Ψ for different shapes nanoparticles

Model	Platelet	Blade	Cylinder	Brick
Ψ	0.52	0.36	0.62	0.81

Table 3: Thermophysical properties of water and nanoparticles

Model	$\rho(kgm^{-3})$	$c_p(kg^{-1}K^{-1})$	$k(Wm^{-1}K^{-1})$	$\beta \times 10^{-5}(K^{-1})$
Pure water(H_2O)	997.1	4179	0.613	21
Copper(Cu)	8933	385.0	401.0	1.67

Following Cogley et al.(1968) for optically thin fluid with relatively low density, the heat flux is expressed as;

$$\frac{\partial q_r}{\partial y}=-4\alpha^2(T'-T_0) \quad (5)$$

The symbol α denotes the mean radiation absorption coefficient.

Now introducing equation (5) into equation (2), it yields;

$$\left(\rho c_p\right)_{nf}\left(\frac{\partial T'}{\partial t'}+v'\frac{\partial T'}{\partial y'}\right)=k_{nf}\frac{\partial^2 T'}{\partial y'^2}+4\alpha^2(T'-T_0)-Q_0(T'-T_0) \quad (6)$$

Now we introduce the following dimensionless quantities into equations (1) and (6)

$$x=\frac{x'}{d},y=\frac{y'}{d},u=\frac{u'}{U_0},t=\frac{tU_0}{d},p=\frac{d}{\mu U_0}p',T=\frac{T'-T_0}{T_w-T_0},\omega=\frac{d\omega'}{U_0},\varepsilon=\frac{\mu}{\mu_f},\frac{\partial p}{\partial x}=\lambda e^{i\omega t},$$

$$Re=\frac{U_0 d}{v_f},M^2=\frac{\sigma B_0^2 d^2}{\mu_f},K=\frac{K'}{d^2},Gr=\frac{g\beta_f d^2(T_w-T_0)}{v_f U_0},Pe_t=\frac{U_0 d\left(\rho c_p\right)_f}{k_f},N^2=\frac{4d^2\alpha^2}{k_f},$$

$$\lambda n=\frac{k_{nf}}{k_f},S=\frac{Q_0 d^2}{k_f},\eta=\frac{1}{U_0},v=\frac{v'}{v_0},$$

Together with equations (4a)-(4e) appropriately.

Re is the Reynolds number, M is the magnetic parameter also known as the Hartmann number, K is the permeability, Gr is the thermal Grashof number, Pe is the Peclet number, N is the radiation parameter, S is the heat generation parameter.

A close look at the continuity equation shows that the suction velocity normal to the channel is a function of time and shall therefore be taken as;

$$v' = v_0(1 + \epsilon A e^{nt}) \quad (7)$$

The following were obtained;

$$m_4 Re\left(\frac{\partial u}{\partial t} - m_2\frac{\partial u}{\partial y}\right) = \lambda e^{i\omega t} + m_5\frac{\partial^2 u}{\partial y^2} + \left(M^2 + \frac{m_5}{K}\right)u + m_6 GrT \quad (8)$$

$$\frac{m_1 Pe}{\lambda n}\left(\frac{\partial T}{\partial t} - m_2\frac{\partial T}{\partial y}\right) = \frac{\partial^2 T}{\partial y^2} + \frac{N^2 - S}{\lambda n}T \quad (9)$$

where $m_1 = 1 - \phi + \phi\frac{(c_p)_s}{(c_p)_f}, m_2 = \eta(1 + \epsilon A e^{nt}), m_5 = 1 + a\emptyset + b\emptyset^2, m_4 = 1 - \phi + \phi\frac{\rho_s}{\rho_f},$

$$m_6 = 1 - \phi + \phi\frac{(\rho\beta)_s}{(\rho\beta)_f}$$

with the boundary conditions as;

y=0; u=0, T=0 (10a)

y=1; u=0, T=1 (10b)

We now assume pertubation solutions for the momentum and temperature of the forms below;

$u(y,t)=u_0(y)+u_1(y)\epsilon e^{i\omega t}$ (11)

$T(y,t)=T_0(y)+T_1(y)\,\epsilon e^{i\omega t}$ (12)

Adopting equations (11) and (12) in equations (8) and (9), we obtain ordinary differential equations depending on the space coordinate only as follows;

$$m_5\frac{d^2u_0}{dy^2} + m_2 m_4 Re\frac{du_0}{dy} - \left(M^2 + \frac{m_5}{K}\right)u_0 = -m_6 Gr\theta_0 \quad (13)$$

$$m_5\frac{d^2u_1}{dy^2} + m_2 m_4 Re\frac{du_1}{dy} - \left(M^2 + \frac{m_5}{K} + m_4 Rei\omega\right)u_1 = -\lambda - m_6 Gr\theta_1 \quad (14)$$

$$\frac{d^2T_0}{dy^2} + \frac{m_2 m_1 Pe}{\lambda n}\frac{dT_0}{dy} + \frac{(N^2 - S)}{\lambda n}T_0 = 0 \quad (15)$$

$$\frac{d^2T_1}{dy^2} + \frac{m_2 m_1 Pe}{\lambda n}\frac{dT_1}{dy} + \frac{(-N^2 + S + m_1 Pei\omega)}{\lambda n}T_1 = 0 \quad (16)$$

The boundary conditions also as;

y=0; $u_0=0, u_1=0, \theta_0 = 0, \theta_1 = 0$ (17a)

y=1; $u_0=0, u_1=0, \theta_0 = 1, \theta_1 = 0$ (17b)

We proceeded to solve equations (13)-(14) together with the appropriate boundary conditions (equation 17a and 17b) and obtained;

$$u_0(y)=D_5 e^{\alpha_5 y} + D_6 e^{\alpha_6 y} + D_7 e^{\alpha_1 y} + D_8 e^{\alpha_2 y} \quad (18)$$

$$u_1(y)=D_{15} e^{\alpha_{11} y} + D_{16} e^{\alpha_{12} y} + D_{17} + D_{18} e^{\alpha_7 y} + D_{19} e^{\alpha_8 y} \quad (19)$$

$$T_0(y)=D_1 e^{\alpha_1 y} + D_2 e^{\alpha_2 y} \quad (20)$$

$$T_1(y)=D_{11} e^{\alpha_7 y} + D_{12} e^{\alpha_8 y} \quad (21)$$

Invoking equations (18)-(19) into equations (11)-(12), we obtained the final solutions for the momentum and energy equations as follows;

$$u(y,t)= D_5 e^{\alpha_5 y} + D_6 e^{\alpha_6 y} + D_7 e^{\alpha_1 y} + D_8 e^{\alpha_2 y} + \epsilon\,(D_{15} e^{\alpha_{11} y} + D_{16} e^{\alpha_{12} y} + D_{17} + D_{18} e^{\alpha_7 y} + D_{19} e^{\alpha_8 y}) e^{i\omega t} \quad (22)$$

$$T(y,t)= D_1 e^{\alpha_1 y} + D_2 e^{\alpha_2 y} + \epsilon(D_{11} e^{\alpha_7 y} + D_{12} e^{\alpha_8 y})\, e^{i\omega t} \quad (23)$$

The constants in the final solutions are clearly stated in the appendix

It is also very crucial to determine the physical effects at the walls of the channel. Hence, we obtain the physical effects by determining the skin friction coefficient and local Nusselt number as follows:

$$C_f = \frac{\rho d^2\tau_w}{{\mu_f}^2} = \left(\frac{du}{dy}\right)_{y=0,1}, \qquad Nu = \frac{dq_w}{k_f(T_w - T_0)} = -\left(\frac{d\theta}{dy}\right)_{y=0,1},$$

where $\tau_w = \mu_f\left(\frac{du}{dy}\right)_{y=0,d}, q_w = -k_f\left(\frac{dT}{dy}\right)_{y=0,d}$

III. ENTROPY GENERATION

The underlying irreversibility in a channel flow of a nanofluid arise owing to the exchange of momentum and exchange imbedded in the fluids and at the solid boundaries. Therefore, the production of entropy may occur as a result of fluid friction, magnetic field, porosity and heat transfer in the direction of finite temperature gradient. Following Baag et al.(2017) and Bejan(1996); the local volumetric rate of entropy generation in the presence of magnetic field is given by;

$$E_G = \frac{K_{nf}}{T^2}\left(\frac{\partial T'}{\partial y'}\right)^2 + \frac{\mu_{nf}}{T}\left(\frac{\partial u'}{\partial y'}\right)^2 + \frac{\sigma\beta_0^2 u'^2}{T} + \frac{\mu_{nf}}{TK'}u^2 \quad (24)$$

The first term in equation (12) depicts the heat transfer irreversibility, the second and thirds term represent irreversibility due to fluid friction and Lorentz force and the fourth term is the irreversibility due to the presence of porous media. The dimensionless form of equation (24) of local entropy generation rate is given as:

$$Ns=\frac{T_0^2 d^2 E_G}{k_{nf}(T_w - T_0)^2}=\left(\frac{\partial T}{\partial y}\right)^2 + \frac{Br}{\Omega\lambda n}\left[m_5\left(\frac{\partial u}{\partial y}\right)^2 + \left(M^2 + \frac{m_5}{K}\right)u^2\right] \quad (25)$$

Where $\Omega = \frac{(T_w - T_0)}{T_0}$ is the temperature difference parameter, $\chi = \frac{(C_w - C_0)}{C_0}$ is the concentration difference, Md=$\frac{DT_0(C_w - C_0)}{k_f(T_w - T_0)}$ is the interaction between temperature and concentration parameter, Br=EcPr is the Brinkmann number. The Bejan number is expressed as:

$$\text{Be}=\frac{N_1}{N_s} = \frac{1}{1+\Phi} \quad (26)$$

Where$N_s = N_1 + N_2, N_1 = \left(\frac{\partial T}{\partial y}\right)^2 (Heat\ transfer\ irreversibility), N_2 = \frac{Br}{\Omega\lambda n}\left[m_5\left(\frac{\partial u}{\partial y}\right)^2 + \right.$
M2+m5Ku2Irreversibility due to viscous dissipation, Lorentz force and porous media

From equation (26), it is seen that the Bejan number(Be) ranges from $0 \leq Be \leq 1$. Be=1 is the limit at which the heat transfer irreversibility dominates, Be=0 is the opposite limit at which the irreversibility is dominated by fluid friction, Lorentz and porous media effects and Be=0.5 is the case that the heat transfer and fluid friction, Lorentz and porous media entropy generation rates are equal.

IV. RESULTS AND DISCUSSION

Figure 1 shows the effect of Peclet number variation on the temperature. The increase in the Peclet number shows no significant change in the temperature. Figure 2 displays the effect of radiation parameter on the temperature. Increasing the radiation parameter decreases the temperature of the fluid. This is because high radiation of fluid temperature consequently reduces the temperature when it is radiating heat at higher level. Figure 3 depicts the heat generation parameter increase the temperature profile on the increase of heat generation. Figure 4 shows the effective thermal conductivity. Increasing the thermal conductivity increases the fluid temperature. Figure5 depicts the volume fraction of copper nanoparticles. Increase in the volume fraction nanoparticles did not consequently change the temperature of the fluid. Figure 6 presents the increase in the Peclet number increases the velocity of the fluid. The radiation parameter decreases the velocity of the fluid as shown in figure 7 due to a decrease in the momentum boundary layer. Variation in the heat generation and effective thermal conductivity parameters as shown in the figures 8 and 9. Varying the heat generation parameter and effective thermal conductivity did not significantly cause any change in the velocity. Increasing the Reynolds number decreases the velocity of the fluid as shown in figure 10. The presence of Lorentz force in the magnetic field deters the motion of the fluid owing to the friction created by the Lorentz force as displays in figure 11. Increasing the Grashof number increases the velocity of the fluid owing the increase in the thermal buoyancy which in turns increases the boundary layer, hence leading to the increase in the velocity of the fluid as seen in figure 12. The volume fraction of copper nanofluid particles is shown in figure 14. Increasing the volume fraction decreases the fluid velocity. Figure 13 shows no change in the velocity for consequent variation in the porosity on the velocity. Figure 15 shows the impact of the frequency of oscillation on the velocity. Increasing the frequency of oscillation decreases the fluid velocity. The figure 16 shown the different shapes of copper. It is seen that increasing the different shapes of copper increases the velocity of the fluid. The effects of Peclet number, Reynolds number and heat generation parameter on the volume of entropy generation are seen in figures 17, 19 and 21. Increasing the Peclet number causes the volume of entropy generation rapidly increase and decrease at the lower and upper plates respectively. The impacts of the radiation parameter and effective thermal conductivity are clearly stated in figures 18 and 20. It is seen that there are rapid increase and decrease at the upper and lower plate for every consequential increase in the radiation parameter. Increasing the magnetic field parameter, Grashof number, porosity, volume fraction and frequency of oscillation as shown in figures, 23, 24 and 25 yielded no consequential change in the entropy generation. Increasing the different shapes nanoparticles cause a slight increase in the entropy generation as shown in figure 27. The finite temperature difference is displayed in figure 28. It is shown that increasing the finite temperature difference caused a slight decrease in the entropy generation at the lower plate. Lorentz and porous media Lorentz and porous media Figure 29 shows the effect of the Brinkmann number on the entropy generation. It is seen that increasing the Brinkmann number increased the entropy generation slightly at the lower plate. The Brinkmann is a heat source parameter which is a function of joule heating and viscous dissipation. Hence increasing it leads to an increase in the temperature which led to the increase in the entropy generation as seen in the figure 29.

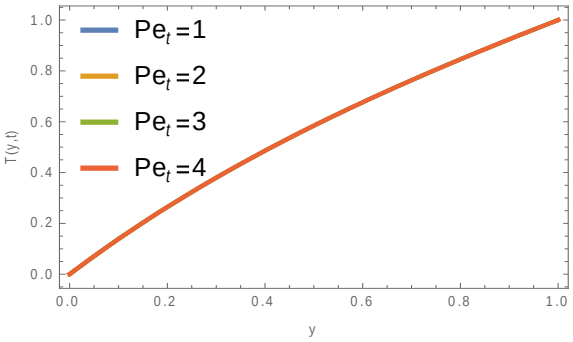

Figure1: Dependence of temperature on coordinate with Peclet number in water based nanofluid when N=1.07, S=0.62, λn=1,t=0.1,$\epsilon = 0.5$

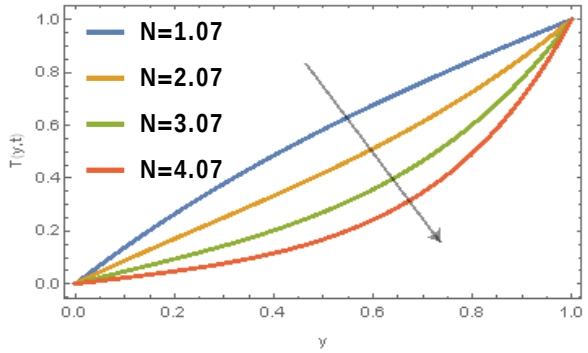

Figure2: Dependence of temperature on coordinate with thermal radiation(N) in water based nanofluid when Pe=1, S=0.62, λn=1,t=0.1,$\epsilon = 0.5$

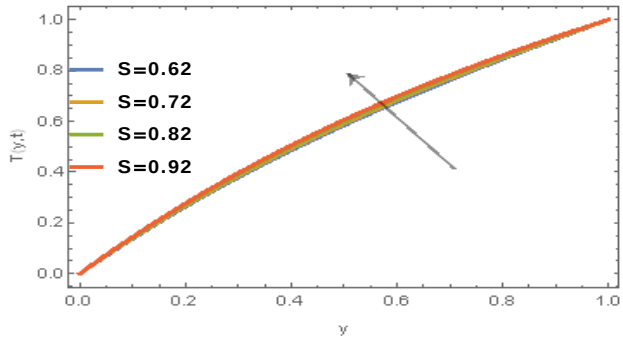

Figure3: Dependence of temperature on coordinate with heat generation parameter in water based nanofluid when N=1.07, Pe=1, λn=1,t=0.1,$\epsilon = 0.5$

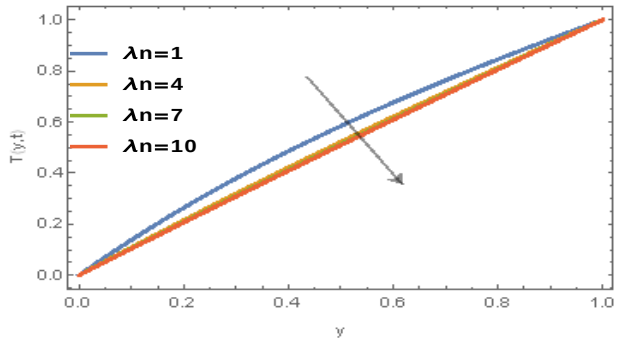

Figure4: Dependence of temperature on coordinate with effective thermal conductivity in water based nanofluid when N=1.07, S=0.62, Pe=1,t=0.1,$\epsilon =$ 0.5

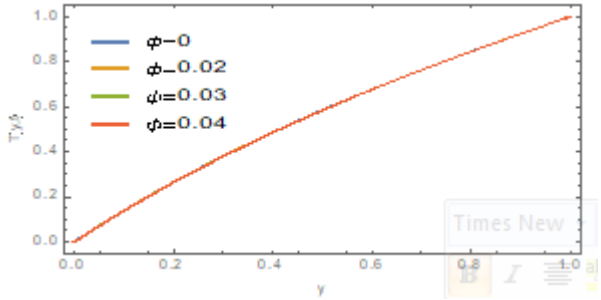

Figure5: Dependence of temperature on coordinate with ϕ of Cu in water based nanofluid when N=1.07, S=0.62, λn=1,t=0.1,$\epsilon = 0.5$

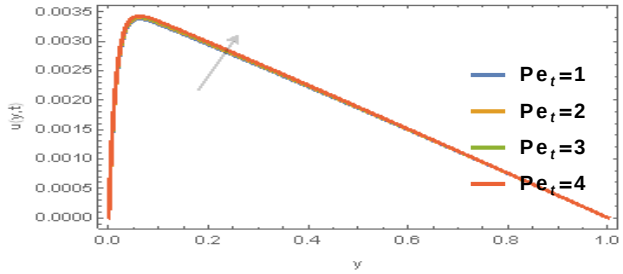

Figure6: Dependence of velocity on coordinate with Peclet number in water based nanofluid when N=1.07, S=0.62, λn=1,t=0.1,$\epsilon =$ 0.5,Gr=0.03,M=0.21,K=1.49,Re=100, $\omega = 0.2$

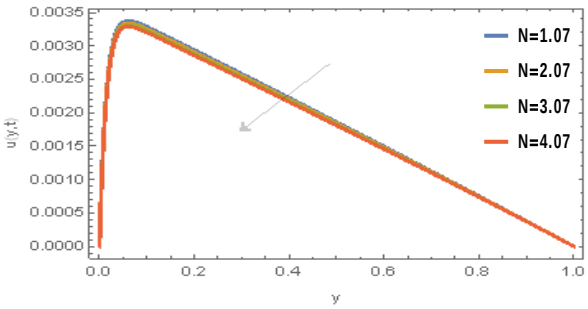

Figure7: Dependence of velocity on coordinate with thermal radiation(N) varying in water based nanofluid when Pe=1, S=0.62, λn=1,t=0.1,$\epsilon =$ 0.5,Gr=0.03,M=0.21,K=1.49,Re=100, $\lambda = 1$, $\omega = 0.2$

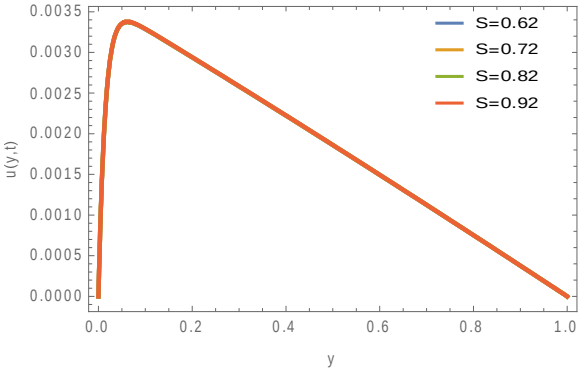

Figure8: Dependence of velocity on coordinate with heat generation parameter varying in water based nanofluid when N=1.07, Pe=1, λn=1,t=0.1,$\epsilon = 0.5$,Gr=0.03,M=0.21,K=1.49,Re=100, $\lambda = 1$, $\omega = 0.2$

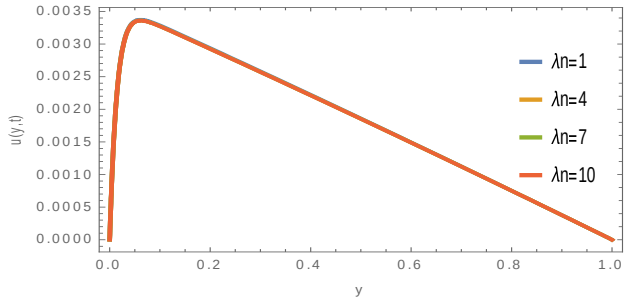

Figure9: Dependence of velocity on coordinate with effective thermal conductivity varying in water based nanofluid when N=1.07, S=0.62,t=0.1,$\epsilon = 0.5$,Gr=0.03,M=0.21,K=1.49,Re=100, $\lambda = 1$,Pe=1, $\omega = 0.2$

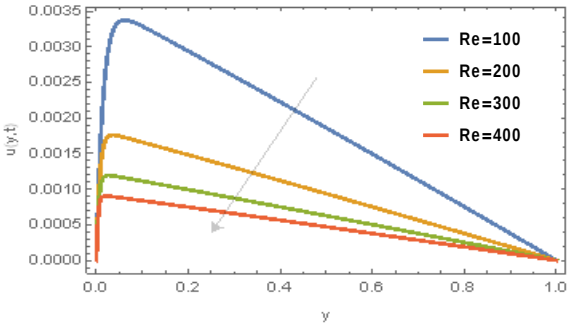

Figure10: Dependence of velocity on coordinate with Reynolds number varying in water based nanofluid when N=1.07, S=0.62, λn=1,t=0.1,$\epsilon = 0.5$,Gr=0.03,M=0.21,K=1.49,Re=100, $\lambda = 1$,Pe=1, $\omega = 0.2$

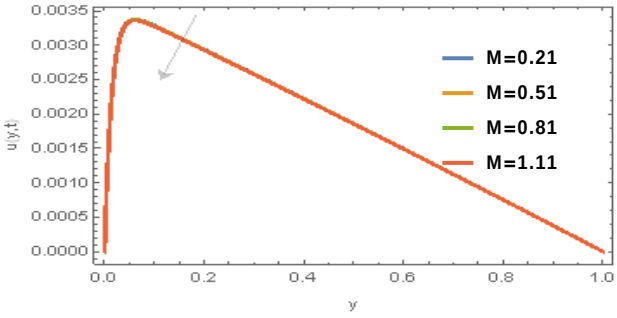

Figure11: Dependence of velocity on coordinate with magnetic field parameter varying in water based nanofluid when N=1.07, S=0.62, λn=1,t=0.1,$\epsilon = 0.5$,Gr=0.03,K=1.49,Re=100, $\lambda = 1$,Pe=1, $\omega = 0.2$

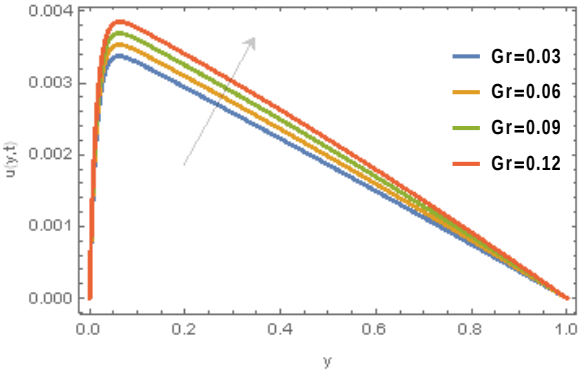

Figure12: Dependence of velocity on coordinate with thermal Grashof number varying in water based nanofluid when N=1.07, S=0.62, λn=1,t=0.1,$\epsilon = 0.5$,M=0.21,K=1.49,Re=100, $\lambda = 1$,Pe=1,m $\omega = 0.2$

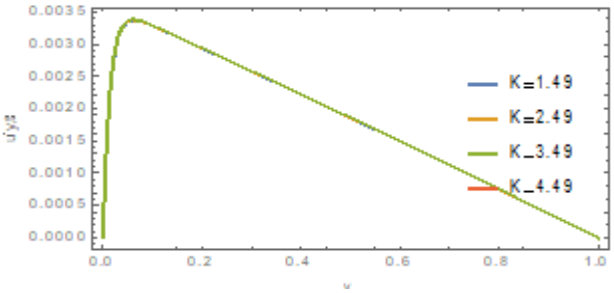

Figure13: Dependence of velocity on coordinate with porosity of the channel varying in water based nanofluid when N=1.07, S=0.62, λn=1,t=0.1,$\epsilon = 0.5$,M=0.21,Gr=0.03,Re=100, $\lambda = 1$,Pe=1, $\omega = 0.2$

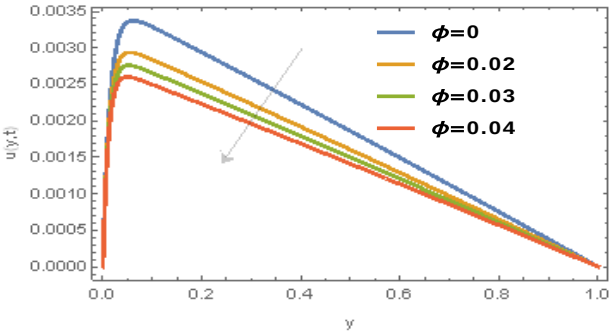

Figure14: Dependence of velocity on coordinate with ϕ of Cu in water based nanofluid when N=1.07, S=0.62,λn=1,t=0.1,$\epsilon = 0.5$,M=0.21,Gr=0.03,Re=100, $\lambda = 1$,Pe=1, $\omega = 0.2$

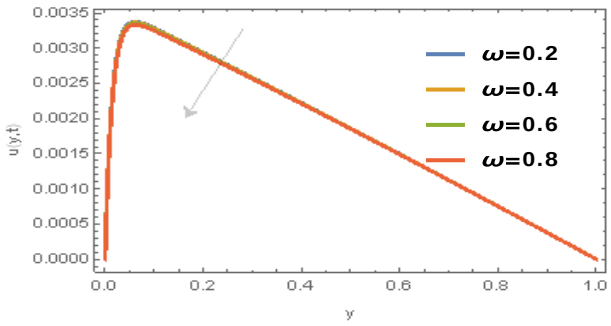

Figure15: Dependence of velocity on coordinate with ω varying in water based nanofluid when N=1.07, S=0.62, λn=1,t=0.1,$\epsilon = 0.5$,M=0.21,Gr=0.03,Re=100, $\lambda = 1$,Pe=1, $\omega = 0.2$

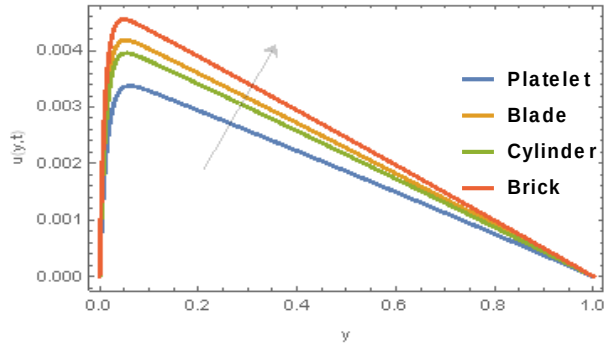

Figure16: Dependence of velocity on coordinate with different shapes of Cu nanoparticles in water- based nanofluid when N=1.07, S=0.62, λn=1,t=0.1,$\epsilon = 0.5$,M=0.21,Gr=0.03,Re=100, $\lambda = 1$,Pe=1, $\omega = 0.2$

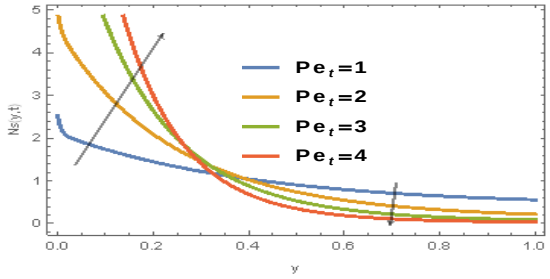

Figure17: Dependence of entropy generation on coordinate with Pe varying in water- based nanofluid when N=1.07, S=0.62, λn=1,t=0.1,ϵ = 0.5,M=0.21,Gr=0.03,Re=100, λ = 1, ω = 0.2

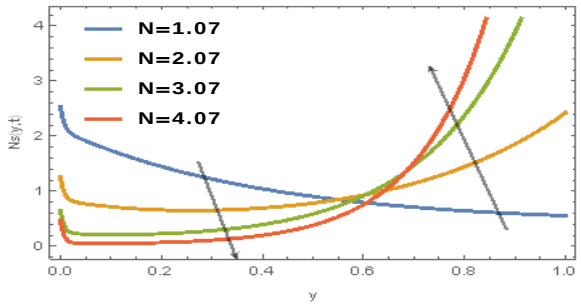

Figure18: Dependence of entropy generation on coordinate with N varying in water- based nanofluid when S=0.62, λn=1,t=0.1,ϵ = 0.5,M=0.21,Gr=0.03,Re=100, λ = 1,Pe=1, ω = 0.2

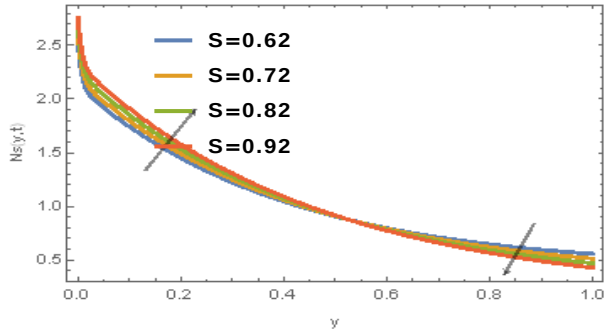

Figure19: Dependence of entropy generation on coordinate with S varying in water- based nanofluid when N=1.07, λn=1,t=0.1,ϵ = 0.5,M=0.21,Gr=0.03,Re=100, λ = 1,Pe=1, ω = 0.2

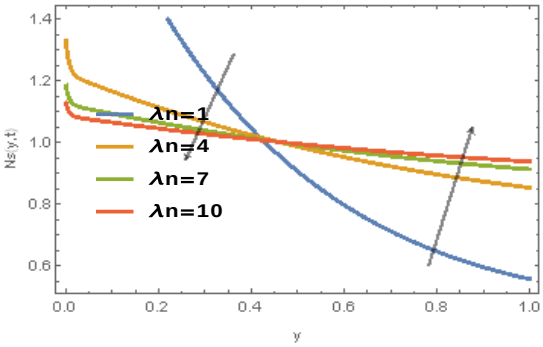

Figure20: Dependence of entropy generation on coordinate with effective thermal conductivity varying in water- based nanofluid when N=1.07, S=0.62,t=0.1,ϵ = 0.5,M=0.21,Gr=0.03,Re=100, λ = 1,Pe=1, ω = 0.2

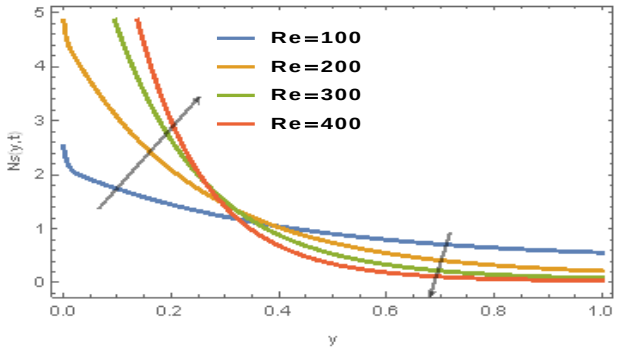

Figure21: Dependence of entropy generation on coordinate with Re varying in water- based nanofluid when N=1.07, S=0.62, λn=1,t=0.1,ϵ = 0.5,M=0.21,Gr=0.03, λ = 1,Pe=1, ω = 0.2

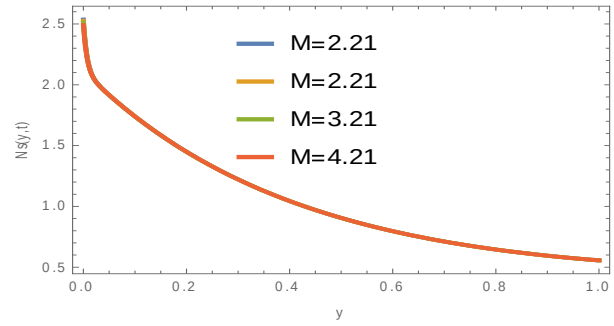

Figure22: Dependence of entropy generation on coordinate with M varying in water- based nanofluid when N=1.07, S=0.62, λn=1,t=0.1,ϵ = 0.5 ,Gr=0.03,Re=100, λ = 1,Pe=1, ω = 0.2

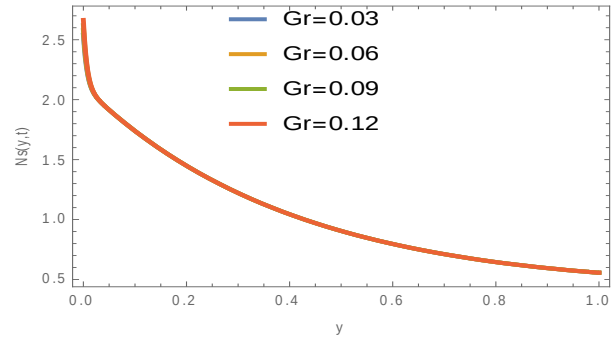

Figure23: Dependence of entropy generation on coordinate with Gr varying in water- based nanofluid when N=1.07, S=0.62, λn=1,t=0.1,ϵ = 0.5,M=1.21 ,Re=100, λ = 1,Pe=1, ω = 0.2

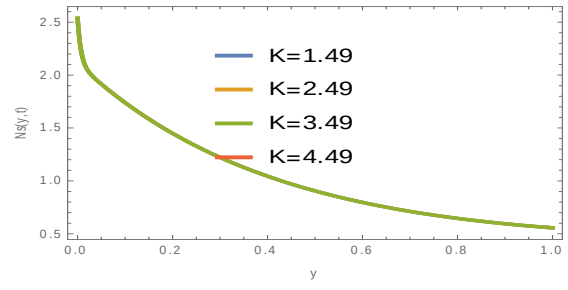

Figure24: Dependence of entropy generation on coordinate with K varying in water- based nanofluid when N=1.07, S=0.62, λn=1,t=0.1,ϵ = 0.5,M=0.21,Gr=0.03,Re=100, λ = 1,Pe=1, ω = 0.2

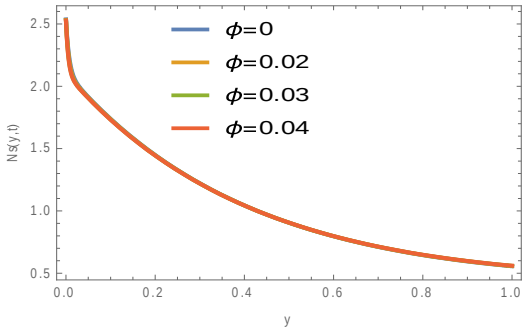

Figure25: Dependence of entropy generation on coordinate with ϕ of Cu in water- based nanofluid when N=1.07, S=0.62, λn=1,t=0.1,ϵ = 0.5,M=0.21,Gr=0.03,Re=100, λ = 1,Pe=1, ω = 0.2,K=1.49,Br=5

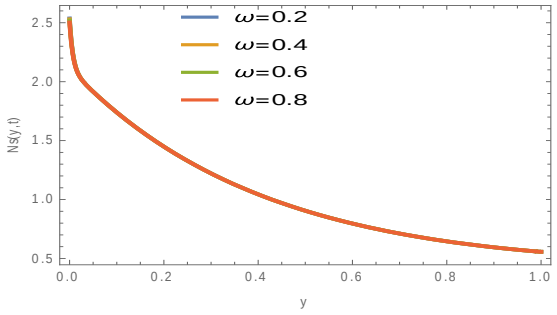

Figure26: Dependence of entropy generation on coordinate with frequency of oscillatioin varying in water- based nanofluid when N=1.07, S=0.62, λn=1,t=0.1,ϵ = 0.5,M=0.21,Gr=0.03,Re=100, λ = 1,Pe=1,K=1.49,Br=5

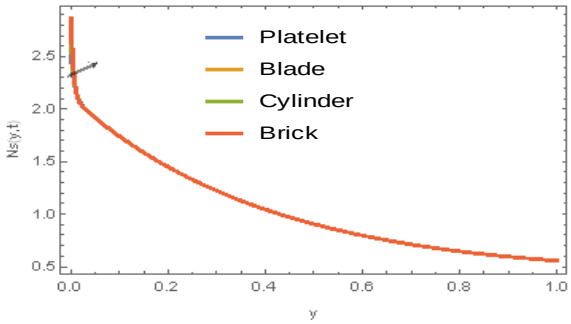

Figure27: Dependence of entropy generation on coordinate with different shapes of Cu nanoparticles in water- based nanofluid when N=1.07, S=0.62, λn=1,t=0.1,ϵ = 0.5,M=0.21,Gr=0.03,Re=100, λ = 1,Pe=1, ω = 0.2, Ω = 1.5,K=1.49,Br=5

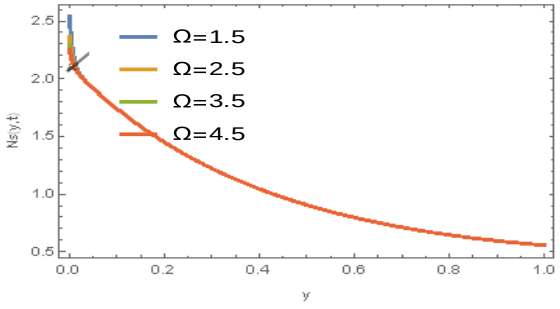

Figure28: Dependence of entropy generation on coordinate with Ω varying in water- based nanofluid when N=1.07, S=0.62, λn=1,t=0.1,ϵ = 0.5,M=0.21,Gr=0.03,Re=100, λ = 1,Pe=1, ω = 0.2,K=1.49,Br=5

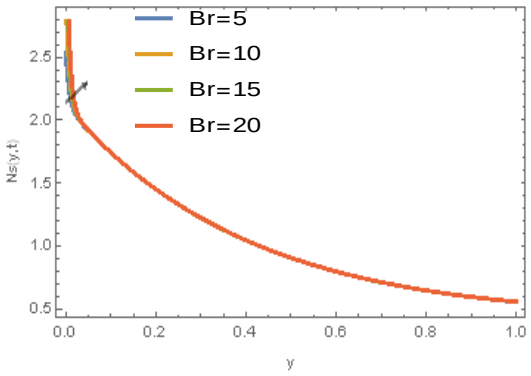

Figure29: Dependence of entropy generation on coordinate with Ω varying in water- based nanofluid when N=1.07, S=0.62, λn=1,t=0.1,ϵ = 0.5,M=0.21,Gr=0.03,Re=100, λ = 1,Pe=1, ω = 0.2,K=1.49, Ω = 1.4

V. CONCLUSION

In this paper, we have successfully analyzed the entropy generation on thermal transfer in MHD natural convection of Cu-H_2O nanofluid in a porous channel with heat generation/absorption. The governing equations were analytically solved and expressed in exponential and complimentary functions. From the foregoing, it is observed that:

1. Thermal radiation decreased the temperature of the fluid.
2. Heat generation/absorption parameter increased the temperature of the fluid.
3. The effective thermal conductivity increased the temperature of the fluid.
4. Peclet number decreased the velocity of the fluid.
5. Reynolds number decreased the fluid velocity.
6. Peclet number, Reynolds number and heat generation rapidly increased and decreased the entropy generation at the lower and upper plates respectively.
7. Brinkmann number increased the entropy generation at the lower plate slightly.

REFERENCE

[1] Aaiza, G.; Khan, I & Shafie, S.(2015). Energy transfer in mixed convection MHD flow of nanofluid containing different shapes of nanoparticles in a channel filled with saturated porous medium. Nanoscale research letters,2(2015), 1-16.

[2] Achogo, W. H.; Adikabu, I. N.; Awortu, I. & Eleonu, B. C.(2020). Soret effect on MHD free convection through a porous inclined channel in the presence of thermal radiation. International journal of research and innovation in applied, 5(7),117-124.

[3] Ajibade, A. O.; Jha, B. K. & Omame, A.(2011). Entropy generation under the effect of suction/injection. Applied mathematical modeling, 35(2011),4630-4646.

[4] Baag, S.; Mishra, S. R.; Dash, G. C. & Acharya, M. R.(2017). Entropy generation analysis for viscoeleastic MHD flow over a stretching sheet embedded in a porous medium. Ain shams engineering journal, 8(2017), 623-632.

[5] Bejan, A.(1996). Entropy generation minimization, second ed., CRC. Boca Raton.

[6] Buggaramulu J. & Venkata M. K.(2017). MHD convection flow of Kuvshinski fluid past an infinite vertical porous plate with radiation and chemical reaction effects. International journal on

recent and innovation trends in computing and communication, 5(9),64-74.

[7] Choi SUS (1995). Enhancing thermal conductivity of fluids with nanoparticle, in: D.A. Siginer, H.P. Wang (Eds.), Developments and Applications of Non- Newtonian Flows. ASME FED, 66(1995),99–105.

[8] Das, S. & Jana, R. N.(2013). Entropy generation due to MHD flow in a porous channel with Navier slip, Ain shams engineering journal, 30(2013),30-40.

[9] Khan, S. M.; Karim, I; Ali, E. L. & Islam, A.(2012). Unsteady MHD free convection boundary – layer flow of a nanofluid along a stretching sheet with thermal radiation and viscous dissipation effects. International nano letters, 2(2012), 1-9.

[10] Latiff, N. A.; Uddin, M. J. & Ismail, A. I.(2016). Stefan blowing effect on bioconvective flow of nanofluid over a solid rotating stretchable disk. Propulsion and power research, 5(4), 267-278.

[11] Makinde, D. O. & Eegunjobi, A.(2013). Entropy generation in a couple stress fluid flow through a vertical channel filled with saturated porous media. Entropy, 15(2013), 4589-4606.

[12] Malvandi, A.; Ganji, D. D.; Hedayati, F & Rad, Y. E.(2013). An analytical study on entropy generation of nanofluids over a flat plate. Alexandria engineering journal, 52(2013), 595-604.

[13] Murugesan, T. & Kumar, D. M.(2019). Viscous dissipation and joule heating effects on MHD flow of a thermo-solutal stratified nanofluid over an exponentially stretching sheet with radiation and heat generation/absorption. World schientific news, 129(2019),193-210.

[14] Naik, M. T. & Sundar, L. S. (2011). Investigation into thermophysical properties of glycol based CuO nanofluid for heat transfer applications. World AcadScience Engineer Technology, 59(2011),,440–446.

[15] Reddy M. G. & Reddy N. B.(2011). Mass transfer and heat generation effects on MHD free convection flow past an inclined vertical surface in a porous medium. Journal of applied fluid mechanics, 4(2), 7-11.

[16] Sharma R. & Isahk, A.(2014). Second order slip flow of Cu-Water nanofluid over a stretching sheet with heat transfer. WSEAS transactions on fluid mechanics, 9(2014), 26-33.

[17] Shateyi, S.; Motsa, S. S. & Makukula, Z.(2015). On spectral relaxation method for entropy generation on MHD flow and heat transfer of a Maxwell fluid. Journal of applied fluid mechanics, 8(1), 21-31.

[18] Srinivasacharya, D. & Bindu H. K.(2015). Entropy generation in a micropolar fluid flow through an inclined channel. Alexandria engineering journal, 55(2016), 973-982.

[19] Vajjha, R.S. & Das, D.K. (2009). Experimental determination of thermal conductivity of three nanofluids and development of new correlations. International journal of heat and mass transfer,, 52(2009), 4675-4682.

APPENDIX

$$\alpha_1 = \frac{\frac{-m_2 m_1 Pe}{\lambda n} + \sqrt{\left(\frac{m_2 m_1 Pe}{\lambda n}\right)^2 - 4\left(\frac{N^2 - S}{\lambda n}\right)}}{2}, \alpha_7 = \frac{\frac{-m_2 m_1 Pe}{\lambda n} + \sqrt{\left(\frac{m_2 m_1 Pe}{\lambda n}\right)^2 - 4\left(\frac{m_1 Pei\omega - N^2 + S}{\lambda n}\right)}}{2},$$

$$\alpha_2 = \frac{\frac{-m_2 m_1 Pe}{\lambda n} - \sqrt{\left(\frac{m_2 m_1 Pe}{\lambda n}\right)^2 - 4\left(\frac{N^2 - S}{\lambda n}\right)}}{2}, D_{11} = D_{12} = 0, \alpha_{11} = \frac{-m_2 m_4 Re + \sqrt{(m_2 m_4 Re)^2 - 4\left(M^2 + \frac{m_5}{K} + m_4 Rei\omega\right)}}{2m_5},$$

$$\alpha_8 = \frac{\frac{-m_2 m_1 Pe}{\lambda n} - \sqrt{\left(\frac{m_2 m_1 Pe}{\lambda n}\right)^2 - 4\left(\frac{m_1 Pei\omega - N^2 + S}{\lambda n}\right)}}{2}, \alpha_{12} = \frac{-m_2 m_4 Re - \sqrt{(m_2 m_4 Re)^2 - 4\left(M^2 + \frac{m_5}{K} + m_4 Rei\omega\right)}}{2m_5}$$

$$D_2 = \frac{1}{e^{\alpha_2 - e^{\alpha_1}}}, D_{18} = \frac{-m_6 Gr D_{11}}{m_5 {\alpha_7}^2 + -m_2 m_4 Re \alpha_7 - \left(M^2 + \frac{m_5}{K} + m_4 Rei\omega\right)}, D_{19} = \frac{-m_6 Gr D_{11}}{m_5 {\alpha_8}^2 + -m_2 m_4 Re \alpha_8 - \left(M^2 + \frac{m_5}{K} + m_4 Rei\omega\right)} D_{17} = \frac{\lambda}{\left(M^2 + \frac{m_5}{K} + m_4 Rei\omega\right)},$$

$$D_1 = \frac{-1}{e^{\alpha_2 - e^{\alpha_1}}}, \alpha_5 = \frac{-m_2 m_4 Re + \sqrt{(m_2 m_4 Re)^2 - 4m_5\left(M^2 + \frac{m_5}{K}\right)}}{2m_5}, \alpha_6 = \frac{-m_2 m_4 Re - \sqrt{(m_2 m_1 Re)^2 - 4m_5\left(M^2 + \frac{m_5}{K}\right)}}{2m_5},$$

$$D_7 = \frac{m_6 Gr A_1}{m_5 {\alpha_1}^2 + -m_2 m_4 Re \alpha_1 - \left(M^2 + \frac{m_5}{K}\right)}, D_8 = \frac{-m_6 Gr A_1}{m_5 {\alpha_2}^2 + -m_2 m_4 Re \alpha_2 - \left(M^2 + \frac{m_5}{K}\right)},$$

$$D_6 = \frac{1}{e^{\alpha_6 - e^{\alpha_5}}}[D_7 e^{\alpha_5 y} + D_8 e^{\alpha_5 y} - D_7 e^{\alpha_1 y} - D_8 e^{\alpha_2 y}], D_5 = \frac{1}{e^{\alpha_6 - e^{\alpha_5}}}[D_7 e^{\alpha_5 y} + D_8 e^{\alpha_5 y} - D_7 e^{\alpha_1 y} - D_8 e^{\alpha_2 y}] - [D_7 + D_8],$$